Petal Color-Transition in Lonicera japonica is Mainly Associated with Increase of the Carotenoid Content and Carotenoid Biosynthetic Gene Expression

Yan Xia
Southwest University https://orcid.org/0000-0001-8239-8099
Weiwei Chen
Southwest University
Weibo Xiang
China Three Gorges Corporation
Dan Wang
Southwest University
Baogui Xue
Southwest University
Xinya Liu
Southwest University
Lehua Xing
Southwest University
Di Wu
Southwest University
Shuming Wang
Southwest University
Qigao Guo (qgguo@126.com)
Southwest University https://orcid.org/0000-0001-9452-3483
Guolu Liang
Southwest University

Research article

Keywords: Lonicera japonica, petal color, carotenoid content, gene expression, endogenous hormones

Posted Date: September 8th, 2020

DOI: https://doi.org/10.21203/rs.3.rs-62167/v1

Version of Record: A version of this preprint was published on February 17th, 2021. See the published version at https://doi.org/10.1186/s12870-021-02877-y.

Abstract

Background: Plants have remarkable diversity in petal color through the biosynthesis and accumulation of various pigments. To better understand the mechanisms regulating the petal pigmentation, we used multiple approaches to investigate the changes of carotenoids, gene expression dynamics and endogenous hormones in *Lonicera japonica* during petal color transitions, i.e. green bud petal (GB_Pe), white flower petal (WF_Pe) and yellow flower petal (YF_Pe).

Results: Metabolome analysis showed that YF_Pe had a much higher content of carotenoids than white petals, with violaxanthin identified as the major carotenoid compound in YF_Pe. Comparative transcriptome analysis revealed that the key differentially expressed genes (DEGs) involved in carotenoid biosynthesis, such as *phytoene synthase*, *phytoene desaturase* and *ζ-carotene desaturase*, were significantly up-regulated in YF_Pe. However, expression levels of the carotenoid degradation-related genes, including *abscisic-aldehyde oxidase 3* and *carotenoid cleavage dioxygenase 4*, were significantly down-regulated in YF_Pe. The results indicated that upregulated carotenoids concentrations and carotenoids biosynthesis-related genes promote the color transition. Furthermore, enrichment analysis of DEGs was mainly associated with the metabolic pathways of hormone signal transduction during petal color transitions. The DEGs were mainly involved in the auxin, cytokinin, gibberellin (GA), brassinosteroid (BR), jasmonic acid and abscisic acid (ABA) signal pathways. Accordingly, analyses of changes in indoleacetic acid, zeatin riboside, GA, BR, methyl jasmonate and ABA levels indicated that the color transitions are regulated by endogenous hormones.

Conclusion: Our results provide new insight into the regulatory mechanisms underlying the petal color transitions during flower development process in *L. japonica*.

Background

Different plant lineages have adopted various mechanisms of flower color determination for the requirements of pollinator attraction or non-pollinator-related traits [1]. Due to the importance of color formation in angiosperms, especially in ornamentals, the biosynthesis pathways of pigments in color formation have been extensively reported [2–6]. Three major classes of pigments, including flavonoids, carotenoids and chlorophylls, are distributed ubiquitously in plants. Among them, flavonoids, such as anthocyanins, are major pigmentation compounds in flowering plants [5]. The carotenoids are also widely taken part in the yellow-to-red coloration of flowers [7]. Chlorophylls, which are a class of essential photosynthetic components, are existed in almost all plants and mainly involved in the formation of green color in flowers [8]. Moreover, flavonoids and carotenoids are often co-existed simultaneously and their combination causes the diversity of flower color [9].

Flower color formation, which mainly involved in biosynthetic pathways of flavonoids and carotenoids, has been extensively studied [2]. The biosynthetic pathway and genes of flavonoids have been best characterized and are associated with many of color formation in flowers [5, 9, 10]. As one of the main

subgroup of flavonoids, anthocyanins mainly caused the color formation of the red, orange, blue and purple in flower colors [5]. Meanwhile, the coloration of flavonoid is greatly depended on the modification with various moieties, including glycosyl, hydroxyl, acyl and methyl groups, in versatile ways resulting in several thousand structures [9]. Carotenoids, a kind of C_{40} isoprenoids, are distributed in some flowers and provide distinct colors ranging from yellow/orange to red [3, 4]. In the initial steps of carotenoid biosynthetic pathway, key enzymes have been well characterized, including *phytoene synthase* (*PSY*), *phytoene desaturase* (*PDS*) and *ζ-carotene desaturase* (*ZDS*) [11–13]. Although the biosynthetic pathways of flavonoids and carotenoids have been well established, the expression dynamics of flavonoids and carotenoids-related genes remain poorly understood during petal color transition in a single flower.

Changes of flower color are comprehensively regulated by physiological changes and transcriptional level fluctuations of related genes. To date, high resolution mass spectrometry (MS)-based metabolome provides an effective technique to detect the accumulation and dynamic changes of metabolites [14–16]. Furthermore, transcriptome analysis has developed into a powerful approach to provide abundant sequence resources for studying the mechanism regulating flower color formation [17, 18]. Changes in the metabolism or transcript level have been reported in flower pigmentations of different varieties using metabolome or transcriptome analysis, but an integrated analysis of metabolism and transcript level in petal color transitions of a single flower have been poorly investigated. To identify the pigments accumulation, endogenous hormone changes and related gene fluctuations in petal color transitions, global analysis of metabolome combined with the transcriptional levels of pigments biosynthesis genes are thus required.

Honeysuckle (*Lonicera japonica* Thunb.), which is known as “gold and silver flower” in China, is widely cultivated in East Asian countries [19, 20]. It has excellent ornamental properties due to its dynamic petal colors of every single flower and provides plant materials for uncovering the molecular mechanisms of petal color transition [21–25]. In our study, we investigated the changes of carotenoid, flavonoids, endogenous hormones and gene expression dynamics in *L. japonica* petals at various stages (i.e. green flower bud, white flower and yellow flower) using the integrated analyses of metabolome, physiology, and transcriptome. With this most extensive analysis of multiple data in *L. japonica* petals, we reveal changes of the key pigments, hormones, and related biosynthesis genes that are associated with petal color transitions.

Methods

Plant materials sampling and color detection

According to previous study [21], flower buds and opening flowers of *L. japonica* were collected from Beijing Botanical Garden, Beijing, China, under permissions. The color of bud/flower gradually changed from green to white and then to yellow during floral development. Three developmental stages of petal, i.e. green bud petal (GB_Pe), white flower petal (WF_Pe) and yellow flower petal (YF_Pe) were selected to

perform pigment metabolome, transcriptome and plant hormone analysis. For each sample, petals were dissected, weighted, sampled, and then frozen immediately in liquid nitrogen and stored at −80 ℃ until used. Then, the color index of petals was measured using a CR-400 chroma meter (Konica Minolta Sensing Inc., Osaka, Japan). Hunter parameters of L*, a* and b* were mainly used according to CIELAB color model.

Carotenoids extraction and quantification

Petal samples from GB_Pe, WF_Pe and YF_Pe were used for carotenoids extraction. Three biological replicates were performed for each developmental stage. Each petal material (~1 g fresh weight) was ground into fine powder, and then dissolved in the solution of n-hexane: acetone: ethanol (2:1:1 (V:V:V)). The solution sample was vortexed (30s), followed by ultrasound-assisted extraction at room temperature in 20 min, and centrifuged at 12,000 g for 5 min to collect the supernatants. Subsequently, the supernatants were evaporated to dry using nitrogen gas stream, then reconstituted in (acetonitrile: methanol = 3:1(V:V)): methyl tert-butyl ether = 85:15 (V:V). Finally, the solution was centrifugated at 12,000 g for 2 min to collect the supernatant for LC-MS/MS analysis. For monitoring the stability of the LC-MS/MS analytical conditions, a quality control (QC) sample was used with equal mixing of all measured samples and was run at intervals during the assay. The stock solutions of standards, which were purchased from Sigma-Aldrich (St. Louis, MO, USA) or Olchemim Ltd. (Olomouc, Czech Republic), were prepared at the concentration of 10 mg/mL in HPLC-grade acetonitrile (ACN), and then were diluted with ACN to working solutions. For each carotenoid, five successive concentration gradients were used to plot the standard curve.

The prepared sample solutions were analyzed by an LC-APCI-MS/MS system (UPLC, Shim-pack UFLC SHIMADZU CBM30A system, www.shimadzu.com.cn/; MS, Applied Biosystems 6500 Triple Quadrupole, www.appliedbiosystems.com.cn/) equipped with an APCI Turbo Ion-Spray interface and operated in a positive ion mode and controlled by Analyst 1.6.3 software (Applied Biosystems Company, Framingham, MA, USA) at Wuhan Metware Biotechnology Co., Ltd. (Wuhan, China). The APCI source operation parameter settings and multiple reaction monitoring (MRM) transitions were performed according to previous study [26]. Finally, the carotenoid levels were calculated according the formula as follows: carotenoid content (μg/g) = A*B/1000/C (A: the carotenoid concentration calculated by standard curve using chromatographic peak area integrals, μg/mL; B: the volume of 75% methanol solution, μL; C: the fresh weight of plant material, g). The SPSS 16.0 was used for the analysis of variance (ANOVA). The differences of means were compared using Duncan's Multiple Range Test.

flavonoids extraction and analyses

Nine petal samples (each sample was parallel to above sample in carotenoids analyses) were used for flavonoids analyses. The freeze-dried petal was crushed into powder by a mixer mill (MM 400, Retsch). Each weighted ~100 mg powder was then extracted overnight at 4 ℃ with 70 % (V/V) aqueous methanol, centrifugated at 10,000 g for 10 min. The supernatant extract was absorbed using a CNWBOND Carbon-GCB SPE Cartridge (250 mg, 3 mL; ANPEL, Shanghai, China) and filtrated through a 0.22 μm SCAA-104

membrane (ANPEL, Shanghai, China). To examine the precision and repeatability of the instrumental assay system and analysis process, the QC sample was prepared by blending all of the samples equally and inserted into test samples at intervals. The prepared samples were analyzed by an LC-ESI-MS/MS system at Wuhan Metware Biotechnology Co., Ltd.. The HPLC conditions and ESI source operation parameters were set according to previous studies [27, 28].

Qualitative and quantitative analyses of flavonoids were basically consistent with the analyses of carotenoids above. Specially, flavonoid identification was performed based on MWDB database (Wuhan MetWare Biotechnology Co., Ltd.) and publicly available metabolite databases following the standard procedures if the standards were unavailable. Flavonoid with statistically significant difference in content was determined with thresholds of |fold change| ≥ 2, *P*-value < 0.05, and variable importance in projection (VIP) ≥ 1.

Determination of various hormones during flower development

The contents of IAA, ZR, GA, BR, MeJA and ABA from GB_Pe, WF_Pe and YF_Pe were measured by an indirect ELISA technique. The extraction, purification and determination of each hormone were performed according to the instructions of the corresponding kit produced by Shanghai Enzyme-linked Biotechnology Co., Ltd. (Shanghai, China). Each stage was prepared by three biological replicates. All data were analyzed for ANOVA by SPSS 16.0, and the differences of means were compared by Duncan's Multiple Range Test.

RNA isolation, cDNA library construction and sequencing

Petal samples of GB_Pe, WF_Pe and YF_Pe were collected and three independent biological replicates were used. Total RNA was extracted from plant tissue using TRIzol reagent (Invitrogen, Carlsbad, CA, USA) following the manufacturer's protocol and digested with DNase I (Takara, Dalian, China). The quality and purity of total RNA were evaluated by a stringent RNA quality control. cDNA library construction and sequencing were performed by the Annoroad Gene Technology (Beijing, China). Each constructed cDNA library (~10 ng) was subjected to paired-end 150 bp sequencing on Illumina HiSeq^{TM} 4000 system (San Diego, CA, USA) according to the manufacturer's instructions.

Data filtering, assembly, and annotation

The raw reads were filtered to remove adapter-polluted reads, low-quality reads with more than 15% $Q \leq 19$ bases (*Q*, Phred Quality Score), and reads with more than 5% ambiguous nucleotides. Subsequently, the *Q*30 of the obtained clean reads were calculated to assess the quality. These clean reads with high-quality were subjected to the following analyses. The Trinity software (http://trinityrnaseq.github.io; [29] was used to perform the de novo transcriptome assembly with its default parameter values.

The assembled unigenes were annotated by homology search to publicly accessible databases (same as those used in Zhao's study (2017)) using local BLAST programs (version 2.2.28) with a significance

threshold of E < 1e-5. Meanwhile, all unigenes were analyzed with Blast2GO (version 3.0.8) to get the gene ontology (GO) annotations [30], which include BP, CC, and MF, with an *E*-value cutoff = 1e-5. The Web Gene Ontology annotation software was adopted to perform GO functional classifications [31]. Furthermore, the sequences were searched against the KEGG database using KEGG Automatic Annotation Server (KAAS) with an E-value threshold < 1e-10.

Differentially expressed genes (DEGs) identification and analysis

The expression level of each unigene was calculated by reads per kilobase millon mapped reads (RPKM) to assess the length and depth of sequencing [32]. Then, the differences in the expression abundance of each gene between each two compared samples were calculated by software of DESeq 2 (version 1.4.5) [33]. Each resulting *p*-value was adjusted to a *q*-value, following the Benjamini-Hochberg procedure for controlling the false discovery rate [34]. The DEGs were identified with a $q \leq 0.05$ and $|\log2(\text{fold-change})| \geq 1$ as thresholds. Then, the GO and KEGG analyses were considered to be significantly enriched with a $q \leq 0.05$ [35]. A GO functional enrichment analysis was performed using the BiNGO plugin of Cytoscape [36].

Reverse transcription quantitative PCR (RT-qPCR) Analysis

A 2 μg of total RNA from *L. japonica* petals was reverse transcribed using the M-MuLV Reverse Transcriptase kit (Takara, Japan) and oligo (dT) primers according to the manufacturer's instructions. The diluted cDNA reaction mixture was used as a template in a 20 μl PCR reaction for transcript measurements. The qPCR was carried out in a Bio-Rad CFX96^{TM} Real-Time System. The qPCR programme was initiated with a preliminary step of 94 ℃ for 5 min, followed by 45 cycles of 94 ℃ for 10 s, 56 ℃ for 10 s, 72 ℃ for 10 s. A melting curve was generated for each sample at the end of each run to ensure the purity of the amplified products with temperature change 0.5 ℃/s from 65 ℃ to 95 ℃ and 5 s for each step afterwards for melt curve. For each sample, three biological replicates were used. The gene-specific primers of qPCR were designed according to the selected sequences from RNA-Seq (Table S1). The expression level of *Actin* was applied to normalize the mRNA levels for each sample [21].

Results

Morphology analysis of petal color transitions

Petal color of every single flower was transformed continuously from green to white and then to yellow during flower development in *L. japonica*. Early in the development of floral buds, primary bud with green petal grew into approximate 3.5-cm in length (Fig. 1a). At the early stage of anthesis, the petals turned from green to white (Fig. 1b). Then, the petals gradually transformed into yellow from white before the withering stage (Fig. 1c). During petal color transitions, the petals at the stages of green bud, white flower and yellow flower were selected. Changes of color index of GB_Pe, WF_Pe and YF_Pe were significant differences (Table S2). Value of redness (a*) in GB_Pe, WF_Pe and YF_Pe were -12.36, -0.58 and 1.25,

respectively. Parameter lightness (L*) in WF_Pe was 82.40, which was higher than that in GB_Pe and YF_Pe. Index of yellowness (b*) in the YF_Pe was the highest (42.55).

Carotenoid accumulations in *L. japonica* petals at various stages

To obtain an accurate understanding of the carotenoid accumulation, carotenoid profiling was analyzed in *L. japonica* petals using LC-MS/MS during petal color transitions. A total of 13 carotenoids were detected from GB_Pe, WF_Pe and YF_Pe (Table 1). Most of carotenoids were significantly highly accumulated in YF_Pe. Compared with GB_Pe and WF_Pe, the α-carotene, antheraxanthin, lycopene, zeaxanthin, violaxanthin, γ-carotene, neoxanthin, β-carotene, β-cryptoxanthin and apocarotenal were significantly up-regulated in YF_Pe. Among them, violaxanthin was the major carotenoid compound in YF_Pe. Some carotenoid compounds, such as lycopene, γ-carotene, β-carotene and β-cryptoxanthin were only detected in YF_Pe.

Widely targeted flavonoid profiling of *L. japonica* petals at different stages

To better understand the content changes of flavonoid, quantitative analysis of flavonoids was further performed by LC-MS/MS technology. A total of 41, 43 and 37 significantly differentially accumulated flavonoids were identified in WF_Pe *vs* GB_Pe, YF_Pe *vs* GB_Pe and YF_Pe *vs* WF_Pe comparisons, respectively (Fig. 2a and Table S3). In total, ten anthocyanins were identified in all samples. Among them, pelargonidin, cyanidin, cyanidin O-malonyl-malonylhexoside and delphin chloride were significantly differentially accumulated. Compared with GB_Pe and WF_Pe, pelargonidin and cyanidin was significantly up-regulated in YF_Pe. Specifically, pelargonidin was not detected in GB_Pe. Compared with WF_Pe, the contents of pelargonidin and cyanidin were increased by 2.11- and 2.36-fold in YF_Pe, respectively. However, cyanidin O-malonyl-malonylhexoside and delphin chloride were not detected in YF_Pe (Fig. 2b and Table S3).

Effects of endogenous hormones during petal color transitions

To obtain the changes of endogenous hormones, the concentrations of indoleacetic acid (IAA), zeatin riboside (ZR), GA, BR, methyl jasmonate (MeJA) and ABA were analyzed. During petal color transitions, the concentrations of IAA, ZR, GA, BR and MeJA decreased, but the content of ABA increased (Fig. 3). The IAA concentration decreased significantly from 717.3 $ng \cdot g^{-1}$ FW (GB_Pe) to 191.0 $ng \cdot g^{-1}$ FW (WF_Pe) then to 118.8 $ng \cdot g^{-1}$ FW (YF_Pe). The ZR and GA concentrations were both firstly decreased significantly from GB_Pe to WF_Pe, and then keep stable from WF_Pe to YF_Pe. The BR concentration was highest in GB_Pe. From GB_Pe to YF_Pe, the BR concentration decreased significantly from 9.2 $ng \cdot g^{-1}$ FW in GB_Pe to 7.3 $ng \cdot g^{-1}$ FW in WF_Pe, and then increased slightly to 8.3 $ng \cdot g^{-1}$ FW in YF_Pe. The level of MeJA was firstly decreased significantly from GB_Pe to WF_Pe reaching the lowest level, and then slightly increased from WF_Pe to YF_Pe. However, the ABA concentration increased significantly from 98.0 $ng \cdot g^{-1}$ FW to 205.2 $ng \cdot g^{-1}$ FW from GB_Pe to YF_Pe (Fig. 3).

Sequencing, de novo assembly and annotation

To identify key candidate genes for petal color transitions, RNA sequencing was carried out from GB_Pe, WF_Pe and YF_Pe. Nine cDNA libraries were sequenced and 448 565 884 raw reads were generated. After the data filtering, 408 576 816 (91.1%) clean reads were produced and *Q*30 values were greater than 96.7%. For each sample, clean reads were obtained from 6.6 to 7.1 Gb (Table S4). A total of 69 946 unigenes were generated with average length is 871 bp and an N50 is 1 636 bp (Table S5). Most of unigenes (96.6 %) were generated from 200 to 3 200 bp in length, and 2 383 (3.4%) unigenes were more than 3 200 bp (Fig. S1).

A total of 34 068 assembled unigenes were annotated (Table S6). Based on sequence similarity, 22 662 (32.4 %) unigenes were enriched into three groups (biological process, cellular component and molecular function) based on GO term analysis (Fig. S2). The biological processes were mainly focused on 'cellular process' and 'metabolic process'. The cellular components were mainly involved in 'cell part'. The molecular functions were mainly classified into 'binding' and 'catalytic activity'. KEGG term analysis was used to identify the functional classifications of the unigenes. There were 9 309 (13.31%) unigenes were enriched into 32 KEGG pathway groups, of which 'signal transduction' represented the largest group, followed by 'carbohydrate metabolism', 'translation' and 'folding, sorting and degradation' (Fig. S3).

Identification and analysis of DEGs

To detect alterations in gene expression, transcriptomic analyses of WF_Pe vs GB_Pe, YF_Pe vs WF_Pe and YF_Pe vs GB_Pe were carried out to identify the key DEGs during petal color transition in *L. japonica* (Fig. S4). A total of 29 679 DEGs were identified based on a 2-fold change at $P < 0.05$ (Fig. S4a). The comparison of WF_Pe vs GB_Pe showed a total of 22 932 DEGs were identified, of which 10 013 were up-regulated and 12 919 were down-regulated. In the YF_Pe vs GB_Pe comparison, 18 984 DEGs were identified, of which 8381 were up-regulated and 10 603 were down-regulated. The comparisons of YF_Pe vs WF_Pe showed a total of 12 220 DEGs were identified, of which 5 936 were up-regulated and 6 284 were down-regulated (Fig. S4b).

All identified 29 679 DEGs were further classified into 8 clusters on the basis of expression alteration during petal color transition (Fig. S5a). A total of 3 470 DEGs were classified into two profiles based on expression changes across the three development stages: expression stable and then increased (profile 4) and expression stable and then decreased (profile 3). The opposite change patterns of gene expression during petal color transition from white to yellow, suggesting a tight linkage of these genes with petal color transition in *L. japonica*.

GO enrichment analysis was further performed to investigate biological functions of these 1 897 DEGs (RPKM > 1 in at least one sample from the 3 470 DEGs) that showed higher or lower expression in YF_Pe. The hormone-mediated signaling pathway was significantly enriched in biological process subcategory (Fig. S5b). DEGs involved in hormone-mediated signaling pathway, including *small auxin-up RNA* (*SAUR*) and *PYRABACTIN RESISTANCE1-like* (*PYL*), were significantly differentially expressed between yellow petals and non-yellow petals and seemed the most relevant to the goal of this study.

Enrichment analysis of DEGs involved in hormone-mediated signaling pathway

GO enrichment analysis showed that DEGs were mainly enriched in hormone-mediated signaling pathway. To better investigate hormonal regulation in the color transitions, we analyzed the 67 DEGs (>1 RPKM) that were enriched in the signaling pathways of auxin, cytokinin, gibberellin (GA), brassinosteroid (BR), jasmonic acid (JA), ABA and ethylene in YF_Pe vs GB_Pe and YF_Pe vs WF_Pe (Fig. S6 and Table S7).

In the auxin signaling pathway, 15 DEGs were identified, of which *AUX1*, *TIR1*, *ARF* and *SAUR* genes were significantly downregulated from GB_Pe to YF_Pe, while three *IAA*s were upregulated at WF_Pe (Fig. S6a). A total of 18 DEGs was enriched in the cytokinine signaling pathway, including HKs, HPs, type-B RRs and type-A RRs. All of these DEGs were downregulated from GB_Pe to WF_Pe and YF_Pe (Fig. S6b). Meanwhile, in the GA signaling pathway, *GID1*, *GID2* and *DELLA* genes were identified and significantly downregulated in YF_Pe (Fig. S6c). In the BR signaling pathway, 13 DEGs were identified, most of them were firstly downregulated and then upregulated in the transition. Specifically, the expression of *BRI1*, *BSK*, *BZR1_2*, *CYCD3* and *TCH4* were significantly higher in YF_Pe than in WF_Pe (Fig. S6d). Four DEGs were enriched in the JA signaling pathway, and their expression levels were higher in GB_Pe than in WF_Pe and YF_Pe (Fig. S6e). Furthermore, *JAR1*, *COI-1* and *MYC2* were expressed at higher levels in YF_Pe than in WF_Pe, while *JAZ* was expressed at lower levels in YF_Pe than in WF_Pe. However, seven DEGs were identified in the ABA signaling pathway, including *PYL*, *PP2C*, *SNRK2* and *ABF*, of which *PYLs* and *SNRK2* were significantly upregulated in YF_Pe (Fig. S6f). In the ethylene signaling pathway, five DEGs were identified, of which *EIN3*, *ERS* and *ERF1* were significantly upregulated in YF_Pe (Fig. S6g).

Pigments accumulation regulation ofpetal color transitions

To investigate the pathways of pigments synthesis/degradation during the transitions, expression levels of carotenoid, flavonoid and chlorophyll metabolism-related genes were analyzed. A total of 44 DEGs (>1 RPKM) regulating carotenoid, flavonoid and chlorophyll metabolism were identified and significantly differentially expressed between yellow petals and non-yellow petals (GB_Pe or WF_Pe) (Fig. 4 and Table S7).

In the carotenoid biosynthesis pathway, *PSY*, *PDS* and *ZDS* were significantly upregulated in YF_Pe. However, three carotenoid degradation-related genes, including *carotenoid cleavage dioxygenase 4* (*CCD4*), *CCD7* and *abscisic-aldehyde oxidase 3* (*AAO3*), were significantly downregulated in YF_Pe (Fig. 4a). Meanwhile, expression levels of chlorophyll metabolism-related genes showed significant difference. Among these genes, biosynthesis-related genes, including *glutamyl-tRNA synthetase* (*GltX*), *protoporphyrinogen IX oxidase* (*PPO*) and *chlorophyll synthase* (*CHLG*) were significantly upregulated in GB_Pe. However, *pheophytinase* (*PPH*), *pheophorbide a oxygenase* (*PAO*) and *red chlorophyll catabolite reductasewere* (*RCCR*) were significantly downregulated in GB_Pe (Fig. 4b). In addition, expression levels of flavonoid/anthocyanin biosynthesis-related genes, such as *chalcone synthase 2* (*CHS2*), *flavonoid 3'-monooxygenase* (*F3'H*), *anthocyanidin 3-O-glucoside 5-O-glucosyltransferase* (*UGT75C1*) and

dihydroflavonol 4-reductase (*DFR*), were significantly downregulated in YF_Pe. Meanwhile, *caffeoyl-CoA O-methyltransferase* (*CAMT*) was expressed at lower level in YF_Pe than in GB_Pe (Fig. 4c).

Validation of the expression analysis of key pigment-related genes

A total of ten pigment-related unigenes were randomly selected and identified by RT-qPCR. The expression patterns of these DEGs were corresponded well with the RPKM values obtained by RNAseq (Fig. 5). Pearson correlation analysis showed high correlation coefficients between RNA-seq and RT-qPCR data, suggesting the sequencing data are reliable.

Discussion

Chlorophylls content and chlorophyll biosynthesis-related genes

During the petal color transitions, the changes of chlorophylls concentrations were significantly decreased from green bud to white bud and yellow flower (22). Accordingly, the expression levels of chlorophyll biosynthesis-related genes, including *GltX*, *hemB*, *hemD*, *PPO*, *CAO, HCAR* and *CHLG*, were significantly down-regulated in WF_Pe and YF_Pe (Fig. 4b), suggesting the chlorophyll biosynthesis might be decreased from GB_Pe to YF_Pe. It was reported that *CAO* and *HCAR* regulate the inter-conversion of chlorophyll a and chlorophyll b, referring to as the chlorophyll cycle, and play a crucial role in the processes of greening [37–39]. *CHLG* is involved in the final step in chlorophyll synthesis [40, 41].

Carotenoids content and carotenoids metabolism-related genes

In flowering plants, carotenoids mainly participate in petal color ranging from yellow to red [3]. Several plant lineages have yellow flowers contain pigments derived from carotenoids [5]. In our study, most of carotenoids were significantly up-regulated in YF_Pe compared with WF_Pe (Table 1). Among them, the top five carotenoids were α-carotene, zeaxanthin, violaxanthin, γ-carotene, β-cryptoxanthin. Importantly, γ-carotene and β-cryptoxanthin were only detected in YF_Pe. Similarly, previous study has been reported that the content of total carotenoids dramatically increase from the WF to YF stage [22, 25].

In accordance with the changes of carotenoids content, the carotenoids biosynthesis-related genes, such as *PSY*, *PDS* and *ZDS*, were significantly up-regulated in YF_Pe (Fig. 4a), and were consistent with the previous results [25]. Because of their key roles in regulating carotenoid biosynthesis, *PSY*, *PDS* and *ZDS* have been subjected to intensive investigation. Previously, in the steps of carotenoid biosynthesis, *PSY* is involved in the condensation of two geranylgeranyl diphosphate molecules into phytoene, and the up-regulation of *PSY* is enhanced carotenoid accumulation [42–47]. Then, the phytoene is subjected to a series of desaturation reactions catalyzed by the carotene desaturases, such as PDS and ZDS [4, 43]. The similar observation of petal colors has been reported in monocots, such as *Lilium* and *Oncidium* [7, 48]. In different cultivars of Asiatic hybrid lily, the petal colors are correlated well with the transcription levels of biosynthetic genes, including *PSY*, *PDS* and *ZDS* [48]. In *Oncidium* cultivars, the varied petal colors, such as yellow, orange and white, are involved in differential expression of carotenoid-related genes [7]. In our

study, expression level of carotenoid catabolism-related gene *CCD4* was significantly down-regulated in YF_Pe. As reported for pigments of *Brassica* and *Dendranthema* have shown that the carotenoid content increase is related to disruption of a *CCD4* gene involving the petal color from white to yellow [49, 50]. In the rose cultivars of yellow petals, carotenoid degradation has a high correlation with the expression of *RhCCD4* [51]. It is reported that the function of *CCD4* genes affects the carotenoid level in various plants, but the precise role of the *CCD4* genes in the degradation process of carotenoids in *L. japonica* petals needs more research.

We found that two anthocyanins (pelargonidin and cyanidin) were both significantly up-regulated in YF_Pe. However, another two compounds of cyanidin O-malonyl-malonylhexoside and delphin chloride were both not detected in YF_Pe (Table S3). After anthesis, total content of flavonoids was decreased from silver flowering stage to gold flowering stage [21, 22], while the pH of cytochylema was steady during flower development [22]. Although groups of plant floral tissue could produce anthocyanin and carotenoid pigments simultaneously, the addition of a second pigment provides considerable interactions that may lead one pigment is masked by the other in the tribe Antirrhineae [52].

Herein, the expression levels of some key flavonoids biosynthesis-related genes, such as *CHS2*, *F3'H* and *DFR*, were significantly down-regulated in YF_Pe (Fig. 4c). Previously, *CHS* gene is involved in flavonoids in two species of *Anoectochilus* [53]. The expression level of *F3'H* is associated with flavonoids accumulation in tea and sorghum [54, 55]. As an important step in the flavonoid biosynthetic pathway, *DFR* is associated with anthocyanins coloration in *Brassica rapa* [56].

Changes of hormones concentrations and key hormone signal transduction-related genes

Plant hormones are involved in all stages of flower development. In our study, concentration changes of IAA, ZR, GA, BR, MeJA and ABA revealed that the transition is regulated by endogenous hormones. Accordingly, the key DEGs, which were involved in the pathways of hormone signal transduction, were significantly enriched in auxin, cytokinin, GA, BR, JA, ABA and ethylene signaling pathways.

In this study, the concentration of auxin was significantly decreased from GB_Pe to YF_Pe (Fig. 3a). Accordingly, the genes from auxin signaling pathway were mostly downregulated in YF_Pe (Fig. S6a). For example, *SAUR* genes, a family of auxin-responsive genes in auxin signaling pathways, was downregulated in the transitions. However, compared with WF_Pe, the expression levels of three *IAA*s were significantly downregulated in YF_Pe. It was previously reported that IAA represses the transcripts of carotenoids biosynthesis-related genes, e.g. *PSY*, *ZISO*, PDS and *CRTISO* [57]. This indicated that downregulation of *IAA* gene play important roles in carotenoids accumulation. In the process of flower development, the concentrations of cytokinin and GA remained at high levels in GB_Pe (Fig. 3b, c). This is mainly associated with controlling cell expansion in flowers [58, 59].

Concentrations of BR and MeJA were both slightly higher in YF_Pe than those in WF_Pe (Fig. 3d, e). The expression of most genes from the BR and JA signaling pathways, including *BRI1*, *BSK*, *BZR1_2*, *TCH4*, *CYCD3*, *JAR1*, *COI-1* and *MYC2* were upregulated in YF_Pe (Fig. S6d, e). In *Solanum lycopersicum*,

application of brassinosteroids is previously reported to increase carotenoid accumulation [60]. Furthermore, ectopic expression of *BZR1-1D* is resulted in an increase in carotenoids accumulation [61]. Meanwhile, the exogenous application of MeJA in the *Never ripe* mutant of *Solanum lycopersicum* significantly enhanced the lycopene accumulation, as well as the expression level of *PSY1* and *PDS* [62]. In present study, the expression levels of *PSY* and *PDS* were significantly higher in YF_Pe than in WF_Pe (Fig. 4a).

Genes from the ethylene and ABA signaling pathways were significantly upregulated during petal color transitions (Fig. S6f). For example, *EIN3*, *ERS* and *ERF1*, the genes of ethylene signaling pathway, were upregulated in YF_Pe; *PYL* and *SNRK2* were upregulated in ABA signaling pathway in YF_Pe; the expression level of *ABF* reached the highest level in WF_Pe. Previously, upregulation of ethylene-related genes was accelerated chlorophyll degradation [63]. Su et al. (2015) reported that carotenoid accumulation is controlled by upregulating ethylene-related genes. In our study, the upregulation of *EIN3*, *ERS* and *ERF1* (Fig. S6g) might lead to the chlorophyll degradation and carotenoid accumulation at YF_Pe. Previously, in the ABA signaling pathways, *PYL* is involved in the regulation of ABA level in tomato [64]. In Arabidopsis, overexpression of *ABF* is associated with triggering chlorophyll degradation [65–67].

Conclusions

In this study, the most comprehensive metabolome, hormones, and transcriptome analyses were investigated the petal color transitions in *L. japonica*. Analyses of key candidate genes, metabolites and hormones highlighted the effect of carotenoid, flavonoids/anthocyanins and endogenous hormones; this enabled us to clarify the regulatory mechanisms underlying the transitions. Based on previously published studies and our results, we provide a conceptual model for regulatory network of the transitions in *L. japonica* (Fig. 6). In this model, the existing chlorophyll/carotenoid balance is disturbed, and the genes of chlorophyll degradation and carotenoid biosynthesis are significantly up-regulated with the flower development. The expression changes of genes lead the chlorophylls concentrations are significantly decreased and the carotenoids concentrations are significantly increased. Meanwhile, this developmental process is regulated by endogenous hormones. These key pigments-related genes, pigments and hormones promote the petal color transitions from green to white and then to yellow in *L. japonica*.

Abbreviations

GB_Pe: Green bud petal; WF_Pe: White flower petal; YF_Pe: Yellow flower petal; DEGs: Differentially expressed genes; GA: Gibberellin; BR: Brassinosteroid; ABA: Abscisic acid; JA: Jasmonic acid; QC: Quality control; ACN: Acetonitrile; ANOVA: Analysis of variance; GO: Gene ontology; RPKM: Reads per kilobase millon mapped reads; RT-qPCR: Reverse transcription quantitative PCR; PSY: Phytoene synthase; PDS: Phytoene desaturase; ZDS: ζ-arotene desaturase; SAUR: Small auxin-up RNA; PYL: PYRABACTIN RESISTANCE1-like; CCD: Carotenoid cleavage dioxygenase; AAO3: Abscisic-aldehyde oxidase 3; GltX: Glutamyl-tRNA synthetase; PPO: Protoporphyrinogen IX oxidase; CHLG: Chlorophyll synthase; PPH:

Pheophytinase; PAO: Pheophorbide a oxygenase; RCCR: Red chlorophyll catabolite reductasewere; CHS2: Chalcone synthase 2; F3’H: Flavonoid 3'-monooxygenase; UGT75C1: Anthocyanidin 3-O-glucoside 5-O-glucosyltransferase; DFR: Dihydroflavonol 4-reductase; CAMT: Caffeoyl-CoA O-methyltransferase

Declarations

Ethics approval and consent to participate

All the plant materials used in this study were provided by Beijing Botanical Garden, Chinese Academy of Science. The field experiments were conducted under local legislation and permissions.

Consent for publication

All authors agreed to publish.

Availability of data and materials

These sequence data have been submitted to the SRA database under accession number PRJNA574570. The datasets supporting the conclusions of this article are included within the article and its additional files.

Competing interests

The authors declare that they have no competing interests.

Funding

This work was partially supported by National Natural Science Foundation of China (31800600), Fundamental Research Funds for the Central Universities (XDJK2019AA001 and XDJK2020B058), Innovation Research Group Funds for Chongqing Universities (CXQT19005). The funding bodies were not involved in the design of the study; collection, analysis, or interpretation of data; or manuscript writing.

Author’s contributions

GL and YX conceived the project. GL and QG supervised the project. YX, WC, and WX designed the experiments and analyzed the data. BX measured the color index of petals. DW and BX performed carotenoids extraction and analyses. XL and LX performed flavonoids extraction and analyses. WC and WX performed endogenous hormones extraction and determination. DW and SW performed RNA isolation and RT-qPCR analyses. YX, WC, and QG wrote the manuscript. All authors approved the final draft of the manuscript.

Acknowledgements

Not Applicable.

References

1. Strauss SY, Whittall JB: **Non-pollinator agents of selection on floral traits**. *Ecology and evolution of flowers* 2006:120-138.
2. Meng Y, Wang Z, Wang Y, Wang C, Zhu B, Liu H, Ji W, Wen J, Chu C, Tadege M: **The MYB Activator WHITE PETAL1 Associates with MtTT8 and MtWD40-1 to Regulate Carotenoid-Derived Flower Pigmentation in *Medicago truncatula***. *The Plant Cell* 2019, **31**(11):2751-2767.
3. Nisar N, Li L, Lu S, Khin NC, Pogson BJ: **Carotenoid Metabolism in Plants**. *Molecular Plant* 2015, **8**(1):68-82.
4. Sun T, Yuan H, Cao H, Yazdani M, Tadmor Y, Li L: **Carotenoid Metabolism in Plants: The Role of Plastids**. *Molecular Plant* 2018, **11**(1):58-74.
5. Grotewold E: **The genetics and biochemistry of floral pigments**. *Annual Review of Plant Biology* 2006, **57**(1):761-780.
6. Zhao D, Tao J: **Recent advances on the development and regulation of flower color in ornamental plants**. *Frontiers in Plant Science* 2015, **6**:261-261.
7. Chiou C-Y, Pan H-A, Chuang Y-N, Yeh K-W: **Differential expression of carotenoid-related genes determines diversified carotenoid coloration in floral tissues of *Oncidium* cultivars**. *Planta* 2010, **232**(4):937-948.
8. Wang Z, Shen Y, Yang X, Pan Q, Ma G, Bao M, Zheng B, Duanmu D, Lin R, Larkin RM: **Overexpression of particular MADS-box transcription factors in heat-stressed plants induces chloroplast biogenesis in petals**. *Plant Cell and Environment* 2019, **42**(5):1545-1560.
9. Tanaka Y, Sasaki N, Ohmiya A: **Biosynthesis of plant pigments: anthocyanins, betalains and carotenoids**. *The Plant Journal* 2008, **54**(4):733-749.
10. Ferreyra MLF, Rius SP, Casati P: **Flavonoids: biosynthesis, biological functions, and biotechnological applications**. *Frontiers in Plant Science* 2012, **3**:222-222.
11. Hirschberg J: **Carotenoid biosynthesis in flowering plants**. *Current Opinion in Plant Biology* 2001, **4**(3):210-218.
12. Han Y, Wang X, Chen W, Dong M, Yuan W, Liu X, Shang F: **Differential expression of carotenoid-related genes determines diversified carotenoid coloration in flower petal of *Osmanthus fragrans***. *Tree Genetics & Genomes* 2014, **10**(2):329-338.
13. Moehs CP, Tian L, Osteryoung KW, Dellapenna D: **Analysis of carotenoid biosynthetic gene expression during marigold petal development**. *Plant Molecular Biology* 2001, **45**(3):281-293.
14. Dettmer K, Aronov PA, Hammock BD: **Mass Spectrometry-Based Metabolomics**. *Mass Spectrometry Reviews* 2007, **26**(1):51-78.
15. Bino RJ, Hall RD, Fiehn O, Kopka J, Saito K, Draper J, Nikolau BJ, Mendes P, Roessnertunali U, Beale MH: **Potential of metabolomics as a functional genomics tool**. *Trends in Plant Science* 2004, **9**(9):418-425.

16. Deng C, Li S, Feng C, Hong Y, Huang H, Wang J, Wang L, Dai S: **Metabolite and gene expression analysis reveal the molecular mechanism for petal colour variation in six *Centaurea cyanus* cultivars**. *Plant Physiology and Biochemistry* 2019, **142**:22-33.
17. Lou Q, Liu Y, Qi Y, Jiao S, Tian F, Jiang L, Wang Y: **Transcriptome sequencing and metabolite analysis reveals the role of delphinidin metabolism in flower colour in grape hyacinth**. *Journal of Experimental Botany* 2014, **65**(12):3157-3164.
18. Duan H, Wang L, Cui G, Zhou X, Duan X, Yang H: **Identification of the regulatory networks and hub genes controlling alfalfa floral pigmentation variation using RNA-sequencing analysis**. *BMC Plant Biology* 2020, **20**(1):110.
19. Yan K, Cui M, Zhao S, Chen X, Tang X: **Salinity stress Is beneficial to the accumulation of chlorogenic acids in honeysuckle (*Lonicera japonica Thunb.*)**. *Frontiers in Plant Science* 2016, **7**(e18949):1563.
20. He SQ, Hu QF, Yang GY: **Research of honeysuckle**. *Yunnan Chemical Technology* 2010, **37**(3):72-75 (In Chinese).
21. Wu J, Wang X, Liu Y, Du H, Shu Q, Su S, Wang L, Li S, Wang L: **Flavone synthases from *Lonicera japonica* and *L. macranthoides* reveal differential flavone accumulation**. *Scientific Reports* 2016, **6**(1):19245-19245.
22. Fu L, Li H, Li L, Yu H, Wang L: **Reason of flower color change in *Lonicera japonica***. *Scientia Silvae Sinicae* 2013, **49**(10):155-161 (In Chinese).
23. Li J, Lian X, Ye C, Wang L: **Analysis of Flower Color Variations at Different Developmental Stages in Two Honeysuckle (*Lonicera Japonica* Thunb.) Cultivars**. *HortScience* 2019, **54**(5):779-782.
24. Ren YF, Yong-Ping MA, Wang WL: **Study on the Categories and Contents of the Flower Color Pigments of *Lonicera japonica* Thunb**. *Journal of Anhui Agricultural Sciences* 2015, **43**(2):90-93 (In Chinese).
25. Pu X, Li Z, Tian Y, Gao R, Hao L, Hu Y, He C, Sun W, Xu M, Peters RJ: **The honeysuckle genome provides insight into the molecular mechanism of carotenoid metabolism underlying dynamic flower coloration**. *New Phytologist* 2020:doi: 10.1111/nph.16552.
26. Liu Y, Lv J, Liu Z, Wang J, Yang B, Chen W, Ou L, Dai X, Zhang Z, Zou X: **Integrative analysis of metabolome and transcriptome reveals the mechanism of color formation in pepper fruit (*Capsicum annuum* L.)**. *Food Chemistry* 2020, **306**:125629.
27. Wang D, Zhang L, Huang X, Wang X, Yang R, Mao J, Wang X, Wang X, Zhang Q, Li P: **Identification of nutritional components in black sesame determined by widely targeted metabolomics and traditional Chinese medicines**. *Molecules* 2018, **23**(5):1180.
28. Huang D, Yuan Y, Tang Z, Huang Y, Kang C, Deng X, Xu Q: **Retrotransposon promoter of *Ruby1* controls both light-and cold-induced accumulation of anthocyanins in blood orange**. *Plant, cell & environment* 2019, **42**(11):3092-3104.
29. Grabherr MG, Haas BJ, Yassour M, Levin JZ, Thompson DA, Amit I, Adiconis X, Fan L, Raychowdhury R, Zeng Q: **Full-length transcriptome assembly from RNA-Seq data without a reference genome**. *Nature biotechnology* 2011, **29**(7):644-652.

30. Conesa A, Götz S, García-Gómez JM, Terol J, Talón M, Robles M: **Blast2GO: a universal tool for annotation, visualization and analysis in functional genomics research**. *Bioinformatics* 2005, **21**(18):3674-3676.
31. Ye J, Fang L, Zheng H, Zhang Y, Chen J, Zhang Z, Wang J, Li S, Li R, Bolund L: **WEGO: a web tool for plotting GO annotations**. *Nucleic acids research* 2006, **34**(suppl_2):W293-W297.
32. Mortazavi A, Williams BA, McCue K, Schaeffer L, Wold B: **Mapping and quantifying mammalian transcriptomes by RNA-Seq**. *Nature methods* 2008, **5**(7):621-628.
33. Love MI, Huber W, Anders S: **Moderated estimation of fold change and dispersion for RNA-seq data with DESeq2**. *Genome biology* 2014, **15**(12):550.
34. Storey JD, Tibshirani R: **Statistical significance for genomewide studies**. *Proceedings of the National Academy of Sciences* 2003, **100**(16):9440-9445.
35. Young MD, Wakefield MJ, Smyth GK, Oshlack A: **Gene ontology analysis for RNA-seq: accounting for selection bias**. *Genome biology* 2010, **11**(2):R14.
36. Maere S, Heymans K, Kuiper M: ***BiNGO*: a Cytoscape plugin to assess overrepresentation of Gene Ontology categories in Biological Networks**. *Bioinformatics* 2005, **21**(16):3448-3449.
37. Tanaka A, Ito H, Tanaka R, Tanaka NK, Yoshida K, Okada K: **Chlorophyll a oxygenase (CAO) is involved in chlorophyll b formation from chlorophyll a**. *Proceedings of the National Academy of Sciences* 1998, **95**(21):12719-12723.
38. Kunugi M, Takabayashi A, Tanaka A: **Evolutionary changes in chlorophyllide *a* oxygenase (CAO) structure contribute to the acquisition of a new light-harvesting complex in *micromonas***. *Journal of Biological Chemistry* 2013, **288**(27):19330-19341.
39. Meguro M, Ito H, Takabayashi A, Tanaka R, Tanaka A: **Identification of the 7-Hydroxymethyl Chlorophyll *a* Reductase of the Chlorophyll Cycle in *Arabidopsis***. *The Plant Cell* 2011, **23**(9):3442-3453.
40. Shalygo N, Czarnecki O, Peter E, Grimm B: **Expression of chlorophyll synthase is also involved in feedback-control of chlorophyll biosynthesis**. *Plant Molecular Biology* 2009, **71**(4):425-436.
41. Zhang C, Zhang W, Ren G, Li D, Cahoon RE, Chen M, Zhou Y, Yu B, Cahoon EB: **Chlorophyll synthase under epigenetic surveillance is critical for vitamin E synthesis, and altered expression affects tocopherol levels in Arabidopsis**. *Plant physiology* 2015, **168**(4):1503-1511.
42. Fraser PD, Truesdale MR, Bird CR, Schuch W, Bramley PM: **Carotenoid biosynthesis during tomato fruit development (evidence for tissue-specific gene expression)**. *Plant physiology* 1994, **105**(1):405-413.
43. Moise AR, Al-Babili S, Wurtzel ET: **Mechanistic aspects of carotenoid biosynthesis**. *Chemical reviews* 2014, **114**(1):164-193.
44. Shewmaker CK, Sheehy JA, Daley M, Colburn S, Ke DY: **Seed-specific overexpression of phytoene synthase: increase in carotenoids and other metabolic effects**. *Plant Journal* 1999, **20**(4):401-412.

45. Ducreux LJM, Morris WL, Hedley PE, Shepherd T, Davies HV, Millam S, Taylor MA: **Metabolic engineering of high carotenoid potato tubers containing enhanced levels of β-carotene and lutein**. *Journal of Experimental Botany* 2004, **56**(409):81-89.
46. Ruiz-Sola MA, Rodriguez-Concepcion M: **Carotenoid Biosynthesis in *Arabidopsis*: A Colorful Pathway**. *The Arabidopsis Book* 2012, **10**(10):e0158.
47. Yuan H, Zhang J, Nageswaran D, Li L: **Carotenoid metabolism and regulation in horticultural crops**. *Horticulture research* 2015, **2**(1):15036-15036.
48. Yamagishi M, Kishimoto S, Nakayama M: **Carotenoid composition and changes in expression of carotenoid biosynthetic genes in tepals of Asiatic hybrid lily**. *Plant Breeding* 2010, **129**(1):100-107.
49. Ohmiya A, Kishimoto S, Aida R, Yoshioka S, Sumitomo K: **Carotenoid Cleavage Dioxygenase (CmCCD4a) Contributes to White Color Formation in Chrysanthemum Petals**. *Plant Physiology* 2006, **142**(3):1193-1201.
50. Zhang B, Liu C, Wang Y, Yao X, Liu K: **Disruption of a *CAROTENOID CLEAVAGE DIOXYGENASE 4* gene converts flower colour from white to yellow in *Brassica* species**. *New Phytologist* 2015, **206**(4):1513-1526.
51. Glick A: **Synthesis and Degradation of Carotenoids in Cut Rose Petals during Vase Life, and Characterization of the Effect of Methyljasmonate Treatment on the Processes**. Hebrew University of Jerusalem; 2009.
52. Ellis TJ, Field DL: **Repeated gains in yellow and anthocyanin pigmentation in flower colour transitions in the Antirrhineae**. *Annals of Botany* 2016, **117**(7):1133-1140.
53. Yang L, Zhang JC, Qu JT, He G, Yu HQ, Li WC, Fu FL: **Expression response of chalcone synthase gene to inducing conditions and its effect on flavonoids accumulation in two medicinal species of *Anoectochilus***. *Scientific Reports* 2019, **9**(1):20171.
54. Guo L, Gao L, Ma X, Guo F, Ruan H, Bao Y, Xia T, Wang Y: **Functional analysis of flavonoid 3'-hydroxylase and flavonoid 3',5'-hydroxylases from tea plant (*Camellia sinensis*), involved in the B-ring hydroxylation of flavonoids**. *Gene* 2019, **717**:144046-144046.
55. Mizuno H, Yazawa T, Kasuga S, Sawada Y, Kanamori H, Ogo Y, Hirai MY, Matsumoto T, Kawahigashi H: **Expression of *Flavone Synthase II* and *Flavonoid 3'-Hydroxylase* is associated with color variation in tan-colored injured leaves of sorghum**. *Frontiers in Plant Science* 2016, **7**:1718.
56. Ahmed NU, Park J, Jung H, Yang T, Hur Y, Nou I: **Characterization of dihydroflavonol 4-reductase (*DFR*) genes and their association with cold and freezing stress in *Brassica rapa***. *Gene* 2014, **550**(1):46-55.
57. Su L, Diretto G, Purgatto E, Danoun S, Zouine M, Li Z, Roustan JP, Bouzayen M, Giuliano G, Chervin C: **Carotenoid accumulation during tomato fruit ripening is modulated by the auxin-ethylene balance**. *BMC Plant Biology* 2015, **15**(1):114-114.
58. Ravid J, Spitzer-Rimon B, Takebayashi Y, Seo M, Cna'ani A, Aravena-Calvo J, Masci T, Farhi M, Vainstein A: **GA as a regulatory link between the showy floral traits color and scent**. *New Phytologist* 2017, **215**(1):411-422.

59. Bartrina I, Otto E, Strnad M, Werner T, Schmülling T: **Cytokinin Regulates the Activity of Reproductive Meristems, Flower Organ Size, Ovule Formation, and Thus Seed Yield in *Arabidopsis thaliana***. *Plant Cell* 2011, **23**(1):69-80.
60. Vidya Vardhini B, Rao SSR: **Acceleration of ripening of tomato pericarp discs by brassinosteroids**. *Phytochemistry* 2002, **61**(7):843-847.
61. Liu L, Jia C, Zhang M, Chen D, Chen S, Guo R, Guo D, Wang Q: **Ectopic expression of a *BZR1-1D* transcription factor in brassinosteroid signalling enhances carotenoid accumulation and fruit quality attributes in tomato**. *Plant Biotechnology Journal* 2014, **12**(1):105-115.
62. Liu L, Wei J, Zhang M, Zhang L, Li C, Wang Q: **Ethylene independent induction of lycopene biosynthesis in tomato fruits by jasmonates**. *Journal of Experimental Botany* 2012, **63**(16):5751-5761.
63. Zhang M, Yuan B, Leng P: **The role of ABA in triggering ethylene biosynthesis and ripening of tomato fruit**. *Journal of Experimental Botany* 2009, **60**(6):1579-1588.
64. Kai W, Wang J, Liang B, Fu Y, Zheng Y, Zhang W, Li Q, Leng P: **PYL9 is involved in the regulation of ABA signaling during tomato fruit ripening**. *Journal of Experimental Botany* 2019, **70**(21):6305-6319.
65. Gao S, Gao J, Zhu X, Song Y, Li Z, Ren G, Zhou X, Kuai B: **ABF2, ABF3, and ABF4 Promote ABA-Mediated Chlorophyll Degradation and Leaf Senescence by Transcriptional Activation of Chlorophyll Catabolic Genes and Senescence-Associated Genes in *Arabidopsis***. *Molecular Plant* 2016, **9**(9):1272-1285.
66. Yoshida T, Fujita Y, Sayama H, Kidokoro S, Maruyama K, Mizoi J, Shinozaki K, Yamaguchishinozaki K: **AREB1, AREB2, and ABF3 Are Master Transcription Factors That Cooperatively Regulate ABRE-dependent ABA Signaling Involved in Drought Stress Tolerance and Require ABA for Full Activation**. *Plant Journal* 2010, **61**(4):672-685.
67. Fujita Y, Yoshida T, Yamaguchishinozaki K: **Pivotal role of the AREB/ABF-SnRK2 pathway in ABRE-mediated transcription in response to osmotic stress in plants**. *Physiologia Plantarum* 2013, **147**(1):15-27.

Tables

Table 1. Contents (μg /g FW) of carotenoids in GB_Pe, WF_Pe and YF_Pe

Compounds	GB_Pe	WF_Pe	YF_Pe
α-Carotene	9.54 ± 0.55^{b}	0.00^{c}	20.84 ± 0.54^{a}
Antheraxanthin	0.75 ± 0.00^{b}	0.75 ± 0.00^{b}	1.25 ± 0.04^{a}
Lycopene	0.00^{b}	0.00^{b}	2.15 ± 0. 02^{a}
Zeaxanthin	13.15 ± 0.70^{b}	10.61 ± 0.08^{c}	27.45 ± 1.10^{a}
Violaxanthin	18.87 ± 3.99^{b}	0.60 ± 0.02^{c}	43.81 ± 0.76^{a}
γ-Carotene	0.00^{b}	0.00^{b}	19.97 ± 0.97^{a}
Neoxanthin	14.23 ± 1.31^{b}	1.14 ± 0.04^{c}	18.05 ± 0.21^{a}
β-Carotene	0.00^{b}	0.00^{b}	1.85 ± 0.03^{a}
Lutein	39.30 ± 2.86^{a}	1.46 ± 0.04^{b}	1.09 ± 0.04^{b}
β-Cryptoxanthin	0.00^{b}	0.00^{b}	17.82 ± 0.45^{a}
Astaxanthin	0.00^{c}	1.26 ± 0.00^{a}	1.21 ± 0.00^{b}
Apocarotenal	1.06 ± 0.00^{b}	0.00^{c}	1.07 ± 0.00^{a}
ε-Carotene	0.05 ± 0.00^{a}	0.00^{b}	0.00^{b}

Data are expressed as mean ± SD. Different letters are indicated significant differences at $P<0.05$ (Duncan's multiple range test).

Figures

Figure 1

Morphological observation of L. japonica flowers. a Flower buds with green petals (GB_Pe). b Flowers with white petals (WF_Pe). c Flowers with yellow petals (YF_Pe).

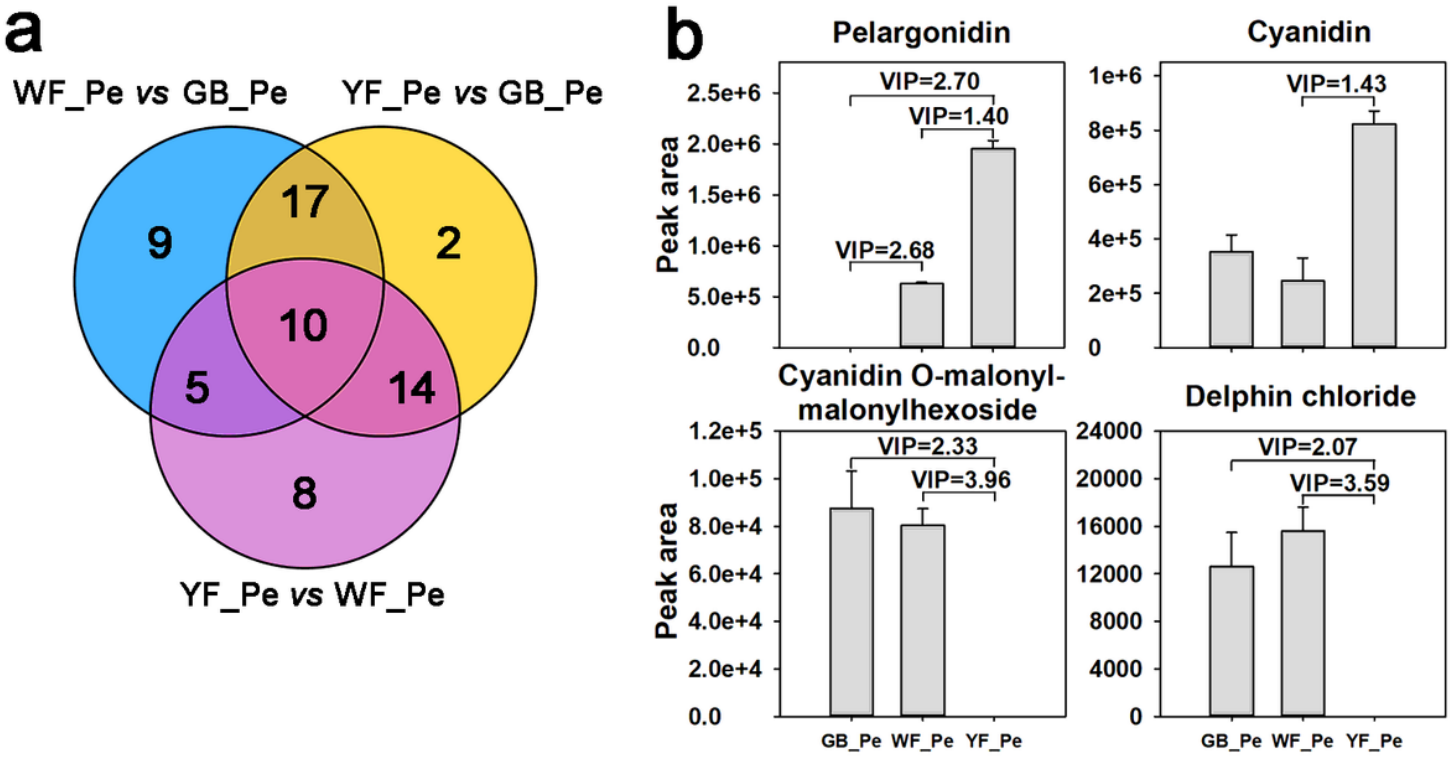

Figure 2

Analyses of flavonoids identified in GB_Pe, WF_Pe and YF_Pe. a Venn diagram analyses of significantly differentially accumulated flavonoids in WF_Pe vs GB_Pe, YF_Pe vs GB_Pe and YF_Pe vs WF_Pe. b Four significantly differentially accumulated anthocyanins in at least one comparison (WF_Pe vs GB_Pe, YF_Pe vs GB_Pe or YF_Pe vs WF_Pe)

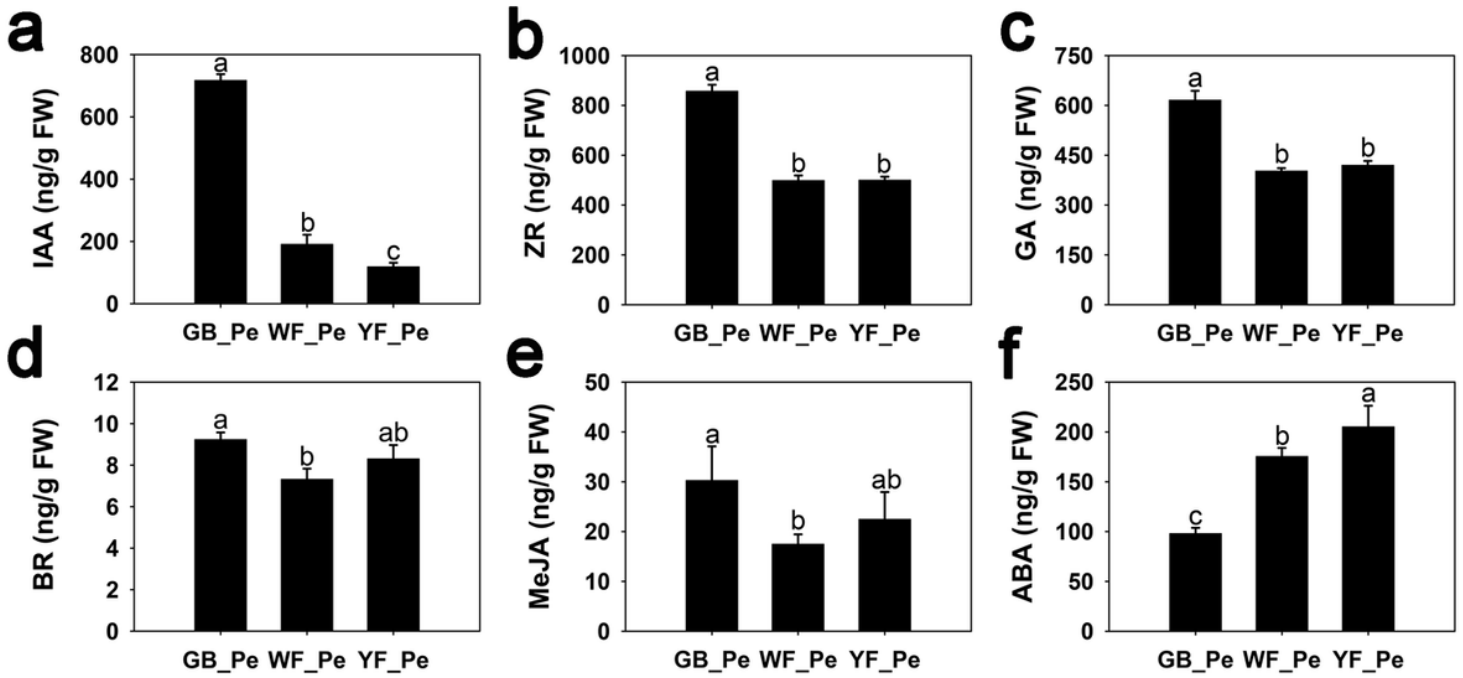

Figure 3

Concentrations of endogenous hormones in petal color transitions in L. japonica. a IAA concentration. b ZR concentration. c GA concentration. d BR concentration. e MeJA concentration. f ABA concentration. Significant differences are indicated by different letters at $P < 0.05$.

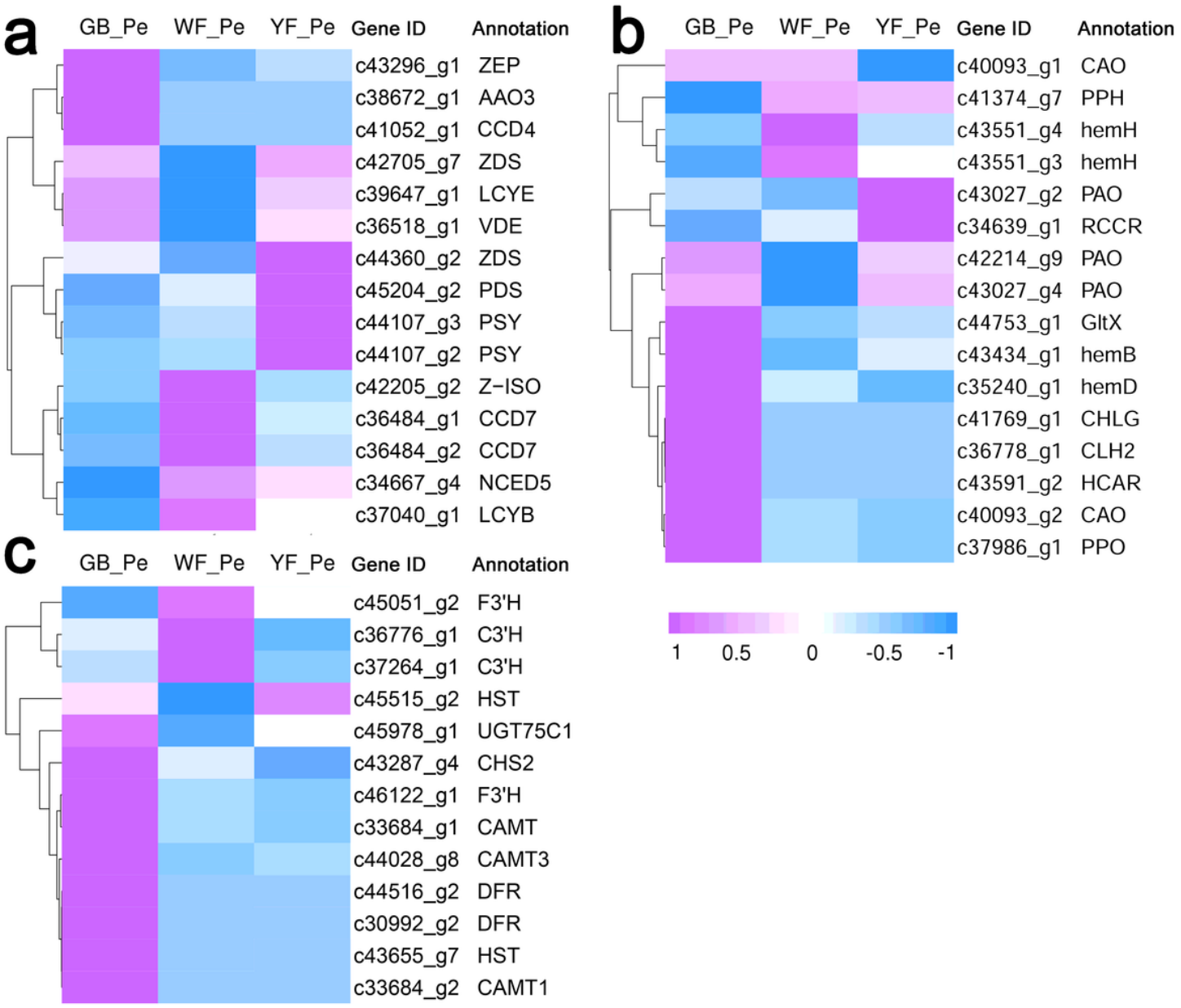

Figure 4

Expression levels of the pigments synthesis/catabolism in GB_Pe, WF_Pe and YF_Pe. a DEGs of carotenoid metabolism-related genes. b DEGs of porphyrin and chlorophyll metabolism-related genes. c DEGs of flavonoid/anthocyanin metabolism-related genes. High expression levels are represented in orchid. Low expression levels are represented in blue.

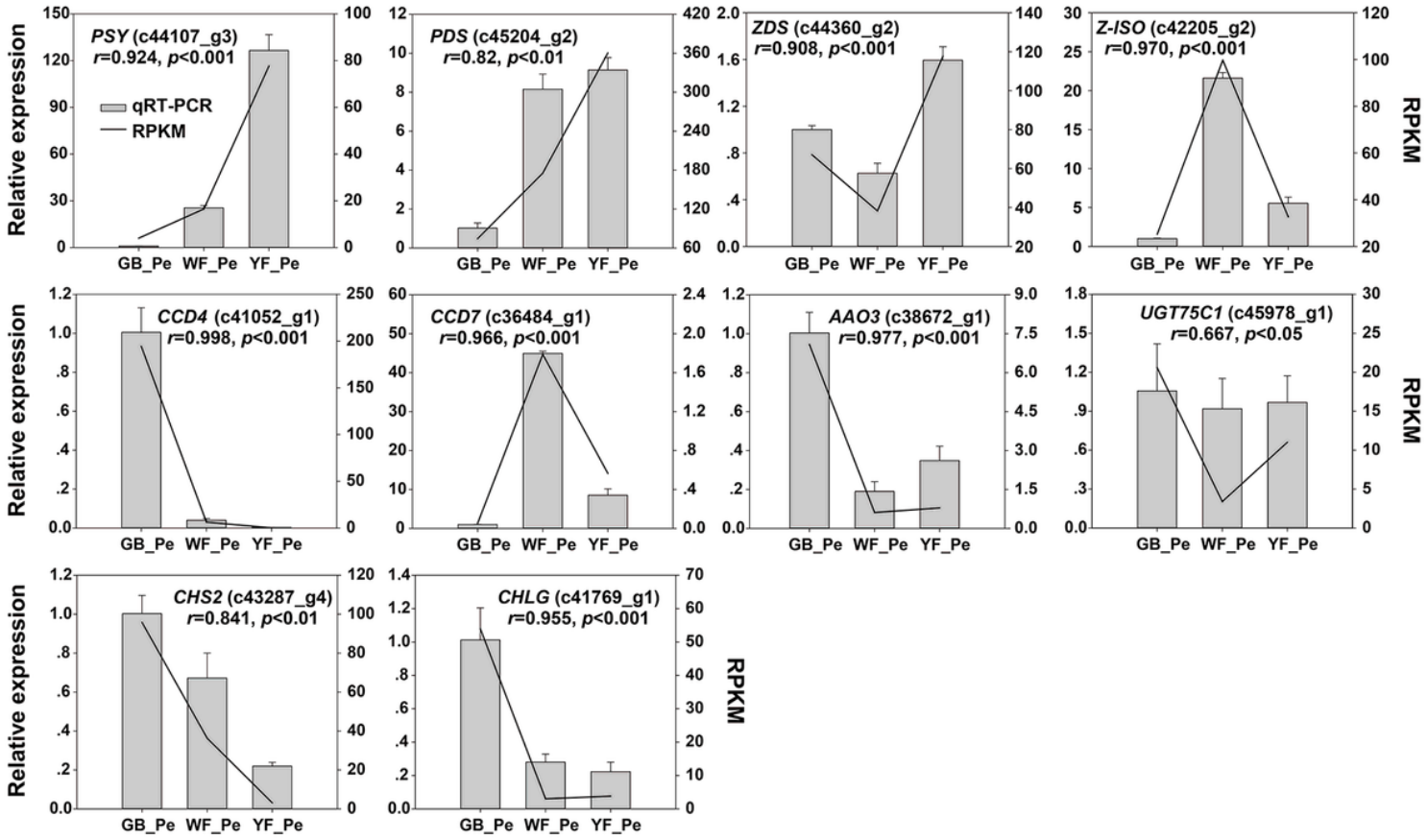

Figure 5

Validation of the expression of pigment-related genes in L. japonica by RT-qPCR. Error bars indicate the standard deviation of three independent biological repeats.

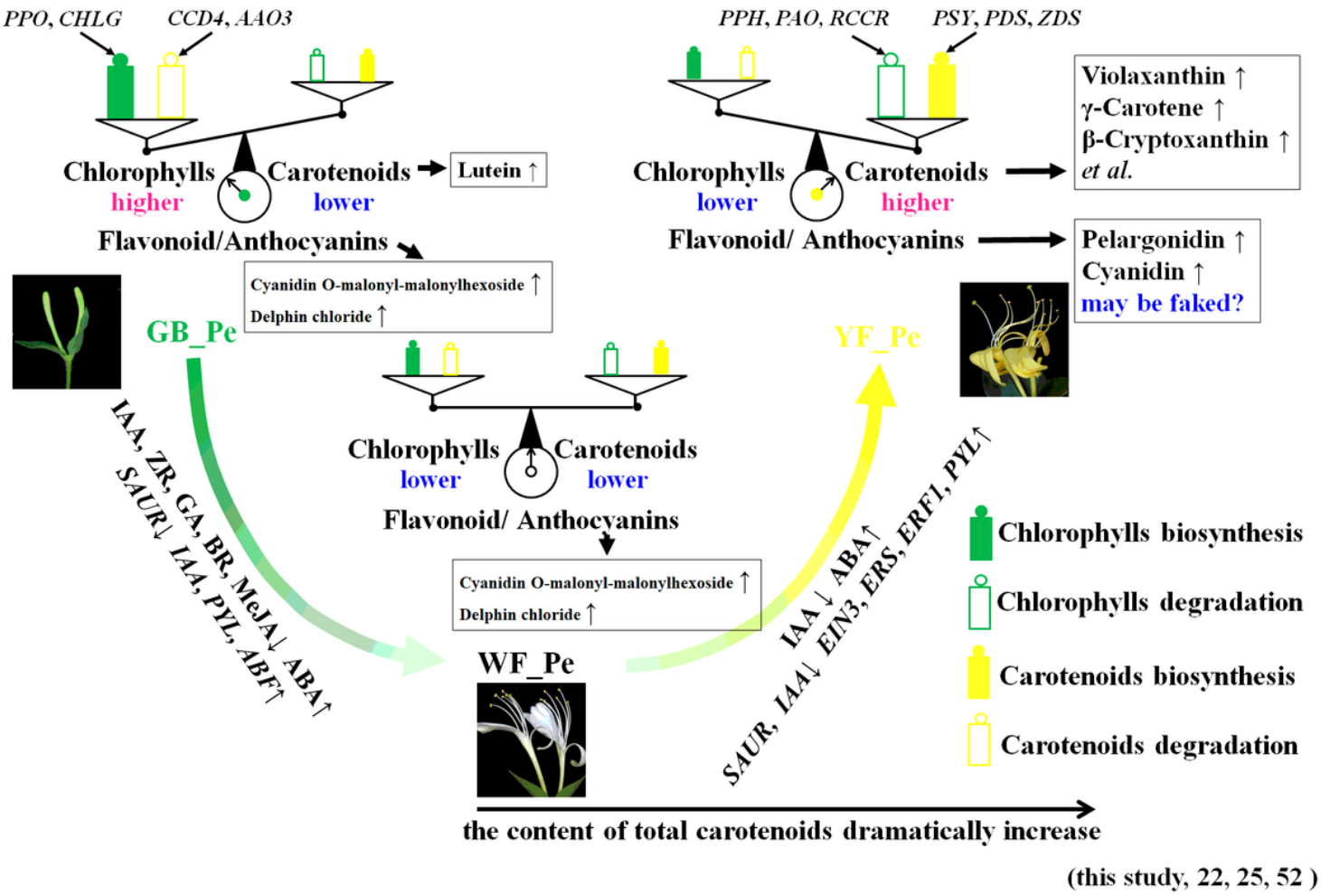

Figure 6

Schematic of changes in the regulatory genes and metabolites in petal color- transition in L. japonica.

Supplementary Files

This is a list of supplementary files associated with this preprint. Click to download.

- FigureS5.tif
- FigureS4.tif
- FigureS3.tif
- FigureS2.tif
- FigureS1.tif
- FigureS6.tif
- TableS7.xlsx
- Supplementarymaterialstables.docx